REPORT DOCUMENTATION PAGE

Form Approved
OMB No. 0704-0188

1. REPORT DATE *(DD-MM-YYYY)*	2. REPORT TYPE	3. DATES COVERED *(From - To)*
28-03-2007	Journal Article	

4. TITLE AND SUBTITLE

Numerical and Experimental Investigation of Microchannel Flows with Rough Surfaces (Preprint)

5a. CONTRACT NUMBER

5b. GRANT NUMBER

5c. PROGRAM ELEMENT NUMBER

6. AUTHOR(S)
T.C. Lilly, J.A. Duncan, & S.L. Nothnagel (USC); S.F. Gimelshein & N.E. Gimelshein
A.D. Ketsdever & I.J. Wysong (AFRL/PRSA)

5d. PROJECT NUMBER

5e. TASK NUMBER
23080532

5f. WORK UNIT NUMBER

7. PERFORMING ORGANIZATION NAME(S) AND ADDRESS(ES)

Air Force Research Laboratory (AFMC)
AFRL/PRSA
10 E. Saturn Blvd.
Edwards AFB CA 93524-7680

8. PERFORMING ORGANIZATION REPORT NUMBER

AFRL-PR-ED-JA-2007-378

9. SPONSORING / MONITORING AGENCY NAME(S) AND ADDRESS(ES)

Air Force Research Laboratory (AFMC)
AFRL/PRS
5 Pollux Drive
Edwards AFB CA 93524-7048

10. SPONSOR/MONITOR'S ACRONYM(S)

11. SPONSOR/MONITOR'S NUMBER(S)
AFRL-PR-ED-JA-2007-378

12. DISTRIBUTION / AVAILABILITY STATEMENT

Approved for public release; distribution unlimited (PA #07386A).

13. SUPPLEMENTARY NOTES
Submitted for publication in Physics and Fluids.

14. ABSTRACT

A conical surface roughness model applicable to particle simulations has been developed. The model has been experimentally validated for channel flows using helium and nitrogen gases at Reynolds numbers from 0.01 to 10 based on inlet conditions. To efficiently simulate gas-surface interaction, molecular collisions with the actual rough surface are simulated by collisions with a randomly positioned conical hole having a fixed opening angle. This model requires only one surface parameter, average surface roughness angle. This model has also been linked to the Cercignani-Lampis scattering kernel as a required reference for use in deterministic kinetic solvers. Experiments were conducted on transitional flows through a 150μm tall, 1cm wide, 1.5cm long microchannel where the mean free path is on the order of the roughness size. The channel walls were made of silicon with: (i) polished smooth surfaces, (ii) regular triangular roughness, and (iii) regular square roughness with characteristic roughness scales of <1μm, 11μm, and 29μm respectively. For the triangular roughness, mass flow reductions ranged from 6% at the higher stagnation pressures tested to 25% at the lower stagnation pressures tested when compared to the smooth channel.

15. SUBJECT TERMS

16. SECURITY CLASSIFICATION OF:			17. LIMITATION OF ABSTRACT	18. NUMBER OF PAGES	19a. NAME OF RESPONSIBLE PERSON
					Dr. Ingrid Wysong
a. REPORT	b. ABSTRACT	c. THIS PAGE			19b. TELEPHONE NUMBER *(include area code)*
Unclassified	**Unclassified**	**Unclassified**	SAR	33	N/A

Equation Chapter 1 Section 1

Numerical and experimental investigation of microchannel flows with rough surfaces. (Preprint)

T. C. Lilly, J. A. Duncan, and S. L. Nothnagel
Dept. of Aerospace and Mechanical Engineering, University of Southern California, Los Angeles, CA 90089

S. F. Gimelshein and N. E. Gimelshein
ERC Inc., Edwards AFB, CA 93524

A. D. Ketsdever and I. J. Wysong
Air Force Research Laboratory, Propulsion Directorate, Edwards AFB, CA 93524

(Received

A conical surface roughness model applicable to particle simulations has been developed. The model has been experimentally validated for channel flows using helium and nitrogen gases at Reynolds numbers from 0.01 to 10 based on inlet conditions. To efficiently simulate gas-surface interaction, molecular collisions with the actual rough surface are simulated by collisions with a randomly positioned conical hole having a fixed opening angle. This model requires only one surface parameter, average surface roughness angle. This model has also been linked to the Cercignani-Lampis scattering kernel as a required reference for use in deterministic kinetic solvers. Experiments were conducted on transitional flows through a 150μm tall, 1cm wide, 1.5cm long microchannel where the mean free path is on the order of the roughness size. The channel walls were made of silicon with: (i) polished smooth surfaces, (ii) regular triangular roughness, and (iii) regular square roughness with characteristic roughness scales of <1μm, 11μm, and 29μm respectively. For the triangular roughness, mass flow reductions ranged from 6% at the higher stagnation pressures tested to 25% at the lower stagnation pressures tested when compared to the smooth channel.

Corresponding Author:
Mr. Taylor C. Lilly
854 W. 36th Pl. RRB 101, Los Angeles, CA 90089
Phone: 213-740-1635 Fax: 213-740-7774 Email: tlilly@usc.edu

I. INTRODUCTION

Surface structure and roughness plays a role, to some extent, in all flow-surface interactions regardless of speed or scale. Traditionally, surface roughness is considered important in low speed micro-flows, where the surface to volume ratio is large and boundary conditions dominate the flow [1]. Since the first report was published, almost a century ago [2], a substantial amount of research on the impact of surface roughness on gas flows in ducts has been accomplished. For instance, the mass flow degradation due to surface roughness was shown numerically and experimentally by Davis et al. [3]. More recently, significant effect of surface roughness on pressure and heat transfer in circular tubes and channels was demonstrated experimentally in Mala and Li [4]. In the experiments by Turner et al. [5] however, the surface roughness was found to have a small effect on gas pressures inside a channel for several pressure ratios. In addition to low speed flows, surface roughness has been seen to cause a noticeable impact on some high-speed flows, such as micro-nozzle expansions [6].

The applicability of continuum numerical approaches, such as those based on the solution of Navier-Stokes equations [7], is limited for flows where the roughness size is smaller than the gas mean free path. There has been work recently on slip conditions to which overcome this limitation [8] In most of the aforementioned applications, the characteristic roughness size is smaller than 1μm, and is usually on the order of or smaller than the gas mean free path. Being essentially a kinetic effect, the interaction of gas molecules with such small surface roughness requires a kinetic numerical approach in order to properly address the gas-surface interaction at the level of molecular velocity distribution functions. Kinetic modeling of surface roughness

effects [9] is hindered by a number of problems, from the accurate representation of complex shapes and roughness patterns to difficulties of experimental validation.

The former has been approached by a number of models, different in their numerical complexity and physical accuracy. Among simplified models are the Cercignani-Lampis (CL) kernel [10][11] and cone model [12][13]. In the CL model, rough surfaces may be simulated by specifying the tangential accommodation coefficient α_t larger than unity [14]. A similar idea was applied by Ketsdever et al. [15] where an anti-specular reflection was introduced. In that model, a fixed fraction of molecules, α, is reflected so that the reflected normal and tangential momentum is the same magnitude as the incoming, but with opposite directions. The models [10] and [15] are easy to implement and may be used with particle as well as deterministic kinetic solvers, but they do not have a clear correlation between the parameters of the models and the physical properties of the rough surface. This drawback was overcome for particle simulations in the cone models [12][13] where the surface is either represented by a number of virtual cones or pre-computed distribution functions are used at the processing stage. These models refer to the actual average angle of the rough surface, although it is hard to use a prescribed angular distribution, and a special cut-off has to be used limiting the number of cones. Another approach is to explicitly specify the rough surface as a set of randomized or regular structures [16]. While this is a reasonable approach for simple geometries, it may be difficult to use for complex, especially three-dimensional, surfaces and roughness structure. Among the more sophisticated, although difficult to implement, roughness models is the fractal model [17][18] and an analytic model [19].

The experimental validation of rough surface models is hampered by requirements of high precision and small scale, both of which increase the difficulty of experimental

measurements, as well as the superposition of different physical effects [20]. Examples of related work on surface roughness are [14] where flow rates through short channels were measured and calculated with a Monte Carlo method, and [21], where triangular roughness in channel flows was studied numerically and experimentally for large Knudsen numbers. Adding to the difficulty of numerical validation is the complexity of relating the measured macro parameters to the micro-phenomenon of interest to the investigation. Although changes in macro-parameters, such as pressure distribution and mass flow, can lead to changes in micro-parameters, such as accommodation coefficient, these macro-parameters do not necessarily indicate specific reasons for the change in accommodation. Changes in angle of incidence [22], gas temperature, surface temperature, surface material, and surface cleanliness can all lead to changes in accommodation. To complicate matters, these parameters can be difficult to quantify experimentally. In addition to the change in accommodation due to the surface, a long microchannel flow may be affected by variation of accommodation with local gas pressure. In most cases, the probability of surface sticking / accommodation decreases as the availability of surface sites decrease. Lundstrom [23] observed the surprising result that Knudsen flow diffusion increased with backing pressure. This was hypothesized to be due to the variation in sticking with local gas density and the tendency of molecules to scatter more specularly off an absorbed wall gas then off the surface.

This study consists of a numerical investigation and experimental validation of the effects of surface roughness. Specifically, the scope will be limited to two-dimensional helium and nitrogen microchannel flows with well-characterized surface roughness. These flows will be in the low Reynolds number regime, based on entrance conditions, with surface rarefaction from near free molecular to near continuum, based on surface roughness. A simple model of the surface roughness that maintains the detailed balance and is applicable to direct simulation

Monte Carlo (DSMC) method has been developed, and its connection to the Cercignani-Lampis scattering kernel is established. This new model is more efficient in both setup cost and simulation time than the direct representation of the physical geometry. It does not exhibit the shortcomings seen in previous simple surface roughness models while being versatile enough to incorporate either an average surface angle or a distribution of surface angles, as well as arbitrary roughness coverage.

II. NUMERICAL APPROACH

A. Conical Model

Molecular collisions with a rough surface can be separated into two stages: (1) a molecule strikes the wall at a particular point and (2) the molecule experiences one or more collisions with the surface roughness feature before leaving the surface. When the characteristic roughness size is significantly less then the mean free path of the gas, no intermolecular collisions occur during the second stage. The time taken for this stage is much smaller then the mean collision time, and the distance traveled is on the order of the roughness size. Therefore, for numerical simulation, the time and distance can be ignored and it is sufficient to specify only the reflected velocity of the molecule after the collision.

To represent this two-stage process in an efficient, yet representative way, a conical model is used to select the reflected velocity of the collided molecule. At the point of collision, the rough surface is represented as a randomly positioned virtual conical hole with fixed opening angle β and height h. The molecule is assumed to enter the cone through the base at point A, as

seen in Figure 1. The collision point for the molecule and the cone wall is then calculated at point B. Here the molecule's reflected velocity is selected assuming a diffuse reflection, although a different reflection model can be used. The process of calculating subsequent collision points and determining post collision velocities is continued until the molecule leaves the cone. The point of origin for the reflected molecule is assumed to be the same as the incoming point of collision; all movement in the virtual cone is only a means for determining the reflected velocity of the colliding molecule. Therefore, the actual value of h is not important (e.g. h=1m can be used). In this algorithm, there are no uncertainties associated with cutoff for very long traveling distances such as those in [12]. Due to surface shape simplification, this algorithm requires only one parameter, the average surface slope (represented as the cone angle β), making it easy to implement in DSMC.

To study the influence of a rough wall, represented by the conical model, on flow properties, examine how the velocity distribution of incident molecules is transformed by collisions with the wall. Consider a distribution of incoming molecules from an equilibrium flow characterized by a Mach number M and directed along the x-axis, assuming the rough surface to be in the xy plane. This scenario has been simulated using the algorithm described above and the distribution of the angle, φ, between the reflected tangential molecular velocity and the flow direction is plotted in Figure 2. Note that the maximum of the distribution corresponds to the direction opposite to the flow, which is generally expected to increase flow resistance.

Verification for the conical surface model has been performed for a two-dimensional thermal bath to assure adherence to detailed balance. The thermal bath constituted helium gas initially heated to 1000K within a 2D box with a surface temperature of 300K. Gas surface

collisions were simulated by the conical roughness model with a cone angle of β=45 deg. The temperature relaxation time inside the test box is illustrated in Figure 3 for a cross section along the centerline. As particles collide with the surface, the temperature decreases from its initial value to the equilibrium value of 300K. By coming to a stable equilibrium the simulation proves adherence to the detailed principle.

B. CL Scattering Kernel

The above stated cone model technique is valuable for particle simulations, but does not have a direct applicability in deterministic kinetic solvers since it is based on individual particle velocities and not on distribution functions. It is reasonable to establish a connection between the conical model and a kernel that is directly applicable to a kinetic solver. One such kernel, the Cercignani-Lampis (CL) [10],[24] scattering kernel, can be used in kinetic solvers but lacks correlation between the physical surface and the main input parameter for the kernel. The conical surface model can be used to relate this parameter, the tangential momentum accommodation coefficient α_t, to an average surface roughness angle.

To facilitate this relation it is necessary to create an analytic expression for the distribution of φ as a function of α_t. Assuming the temperature of the gas and the wall are equal and velocities are normalized by $\sqrt{m/kT}$, the distribution functions of x and y velocity components of incident molecules are

$$f_x^{inc}(v) = \frac{1}{\sqrt{2\pi}} \exp\left(-\left(v - M\sqrt{\gamma}\right)^2 \Big/ 2\right) \tag{1}$$

$$f_y^{inc}(v) = \frac{1}{\sqrt{2\pi}} \exp\left(-v^2/2\right) \tag{2}$$

respectively. After the CL transformation, the x component of the reflected velocity is equal to

$$v_x^{refl} = \frac{1-\alpha_t}{\sqrt{1-\alpha_t}} v_x^{inc} + v_x^{CL} \tag{3}$$

where the distribution function of v_x^{CL} is given by

$$f_x^{CL}(v) = \frac{1}{\sqrt{2\pi\left(1-\left|1-\alpha_t\right|\right)}} \exp\left(-\frac{v^2}{2\pi\left(1-\left|1-\alpha_t\right|\right)}\right) \tag{4}$$

Here, α_t is the CL parameter that corresponds to the tangential accommodation coefficient, $0 \leq \alpha_t \leq 2$. $\alpha_t = 1$ corresponds to zero average tangential momentum relative to the surface; the larger the deviation between α_t and unity, the larger the average momentum of the reflected molecules. Note that v_x^{refl} is the sum of the two independent normally distributed components, therefore, its distribution function can be written as

$$f(v_x^{refl}) = \frac{1}{2\pi} \exp\left(-\left(v_x^{refl} - M\sqrt{\gamma}\frac{1-\alpha_t}{\sqrt{\left|1-\alpha_t\right|}}\right)^2\right) \tag{5}$$

The distribution function of the y velocity component does not change during the CL transformation. Note that $\tan(\phi) = \left|v_y^{refl}\right| / v_x^{refl}$, so for $0 < \phi < \pi/2$ the distribution function of ϕ can be obtained with

$$f(\tan\phi) = \int_0^\infty u_x f_x^{refl}(u_x) f_y^{refl}(u_x \tan\phi) du_x \tag{6}$$

and for $\pi/2 < \phi < \pi$

$$f(\tan\phi) = -\int_{-\infty}^0 u_x f_x^{refl}(u_x) f_y^{refl}(u_x \tan\phi) du_x \tag{7}$$

Finally, the reflected velocity distribution function can be written

$$f_\phi(\phi) = 2 f(\tan\phi)(1+\tan^2\phi) \tag{8}$$

or

$$f_\phi(\phi) = \frac{e^{-t^2}}{\pi} + \frac{t\cos\phi}{\sqrt{\pi}}\exp\left(-t^2\sin^2\phi\right)\left(1+erf\left(t\cos\phi\right)\right) \tag{9}$$

where $t = M\sqrt{\gamma}\left(1-\alpha_t\right)\Big/\sqrt{\left|1-\alpha_t\right|}$

Parameter α_t of the CL transformation can be found by least square fitting of ϕ distributions obtained using the cone reflection algorithm described in section II:A as seen in Figure 2. Figure 4 shows the value of α_t, found by a least square fit, for M=0.3 and different cone angles β. As expected, α_t is maximum at some intermediate value of the cone angle. Since α_t is larger than 1, the average tangential momentum of the reflected molecules points in the opposite direction with respect to the average tangential momentum of the incoming molecules.

The value of α_t only weakly depends on Mach number, as seen in Figure 5, where α_t is shown as a function of Mach number for two different opening angles, β =120º and β =66º. This fact facilitates the use of the CL model in simulations, since the value of α_t can be selected universally depending on the degree of roughness of the surface, and not on the flow properties.

C. Simulation Conditions

In order to validate the conical roughness model and its link to the CL scattering kernel, both were individually incorporated into a DSMC solver and simulations were run for comparison against experiment. To maximize the measurable effect of the different surface models on the flow, the simulations were conducted on a long, narrow microchannel with an L/H = 100 and an assumed infinite width. The 2D capability of SMILE [25] was used in all DSMC computations. This system utilizes the majorant frequency scheme to calculate

intermolecular interactions [26], while using the variable hard sphere model for intermolecular potentials. Four surfaces were used: (i) a fully diffuse smooth surface with complete energy and momentum accommodation, (ii) a smooth surface utilizing the conical surface roughness model with an opening angle of 66º which corresponded to an earlier experimental setup concept, (iii) CL model with a tangential momentum accommodation coefficient of 1.045 attained using the conical model with a 66º cone opening angle, and (iv) a diffuse surface consisting of about 900 triangles representative of an actual experimental shape.

The channel length and half height, from plane of symmetry to the tops of the surface features, were 1.5 cm and 75 μm, respectively. Helium was used as the test gas with stagnation pressure from 200 Pa to 8,000 Pa for all four surfaces. The Knudsen number is defined as

$$Kn = \frac{\lambda}{L} = \frac{1}{\sqrt{2} n \pi d^2 L} = \frac{kT}{\sqrt{2} P \pi d^2 L} \tag{10}$$

where P is the stagnation pressure, k is Boltzmann's constant, T is the stagnation temperature 300K, d is the molecular diameter, and L is the feature size (about 20 μm). The Knudsen number for these tests ranged from 0.1 to 5. Nitrogen was used as the test gas for only surfaces (i) and (ii), with stagnation pressures from 200 Pa to 6,000 Pa. Again, based on the stagnation conditions and the surface roughness size, the Knudsen number ranged from 0.05 to 2. A convergence study was performed to assess the impact of the inflow boundary conditions on the results of the computations. These computations were performed using helium at 6,000 Pa and two inflow boundary locations: the first extending 1700 μm from the channel entrance and 1700 μm from the symmetry plane, the other 850 and 850 μm, respectively. A Maxwellian distribution function with zero flow velocity was assumed at these boundaries. No impact from the boundary location was found. The larger domain was used in all subsequent computations, with the number of molecules ranging from about 1.6 million for the lower pressures to about 10

million for the larger ones. A schematic for the computational domain can be seen in Figure 6, where the outflow boundary condition is modeled as a vacuum.

III. EXPERIMENTAL APPROACH

The experiments were conducted using atomically smooth, triangular patterned, and square patterned silicon textures. Standard microelectromechanical systems (MEMS) processes were performed to create 1 cm by 1.5 cm textured areas centered on 2 cm by 1.5 cm chips. The feature width for both square and triangular textures is approximately 15 μm. The triangles are approximately 11 μm deep with an etched angle of 54.7° from surface parallel, which would give an opening angle of approximately 70°, very close to the numerical simulation. The squares are approximately 30 μm deep, both geometries can be seen in Figure 7. Teflon shims were placed between the chips to create a channel 1 cm wide, 150 μm high, and 1.5 cm long such that gas flow along the length of the channel was perpendicular to the textures etched in the silicon chip. Along this length there were approximately 900 features. This channel was secured in an aluminum holder and dimensions of the channel were measured with a Scanning Electron Microscope before and after testing as seen in Figure 8. The ratio of the measured open area of the channel to the open area of the numerical simulation was used to linearly correct the experimental mass flow data. Typical deviation for the channel height was 3-5%. Deviation for the width was less then 1%.

The aluminum-Teflon-silicon assembly was placed in the wall of a 3550 cm^3 plenum, which acted as a stagnation chamber. The plenum was machined with two gas inlet ports and three ports for pressure measurements. The setup was operated in the CHAFF IV vacuum

chamber at the University of Southern California, which is capable of an ultimate pressure of 10^{-6} Torr with working pressures no higher then 10^{-4} Torr. This allowed plenum pressures from approximately 1 to 100 Torr with ratios of stagnation to ambient pressures greater than 10^5 maintained throughout. Helium or nitrogen test gases were used. Upstream gas flow was measured with a mass flow meter and regulated through a needle valve. The pressure in the plenum was monitored with several differential baratrons. This array of instrumentation allowed measurements of pressure and mass with instrumental precisions below 1%.

IV. RESULTS AND DISCUSSION

The first result to consider is that of the numerical simulation using the smooth, fully diffuse surface with a helium test gas. Figure 9 shows the local pressure, normalized by the stagnation value, and Mach number along the centerline of the channel for plenum pressures of 200 Pa and 2000 Pa. The Knudsen number, based on channel height of 150 μm instead of the feature size, for the 200 Pa case increases from below 1 to about 100. As seen in Figure 9, the pressure in the free molecular flow drops linearly from $P_0 = 200$ Pa to $0.01P_0$ through the channel. The Mach number stays below 0.05 for the majority of the channel, increasing to 1 at the exit; the Mach number for the $P_0 = 2000$ Pa case is higher, as expected. This allows for the use of a constant α_t value in the CL model along the length of the channel.

Figure 10 shows the ratio of local pressure for the conical surface simulation divided by the local pressure for the smooth surface as a function of longitudinal distance down the channel. As expected, the pressure along the channel increases for the rough surface compared to the smooth, since the rough surface impedes the flow. This effect decreases as the flow becomes free molecular, at which point the pressure ratio down the channel asymptotes to 1 far from the

exit. The ratio drops below 1 at the point where the local mean free path exceeds the channel height allowing molecules to "see" the exit without intermolecular collisions. Downstream from this point, any molecules traveling upstream are more likely to leave the channel after colliding with the rough surface than they would be after colliding with a smooth surface. Upstream from this point, molecular collisions are likely to prevent this. Note that a relatively small difference between pressures for the rough and smooth surfaces is observed for much of the channel length, consistent with the measurements of Turner, et al. [5].

Calculated helium mass flow as a function of stagnation pressure is listed in Table 1 for all four surfaces. A reduction in mass flow of 25% at the lower pressures and 6% at higher pressures is seen between the conical surface model and the smooth, fully diffuse case. The CL model with an $\alpha_t = 1.045$ matches the conical model to 7% at the lower pressures and less then 1% at the higher pressures. The conical surface matches the triangular geometry pattern within 3% at the lower pressures and less then 1% at the higher pressures. The impact of the surface roughness is larger for helium then for nitrogen for any given pressure; however, when plotted versus Knudsen number, the impact is similar. Assumptions made for the cone surface model require a non-continuum Knudsen number based on the feature size of the roughness. Although the cone model agrees favorably with the direct representation over the full range tested, it is not a given conclusion that the cone model is applicable in low Knudsen number cases.

There is good agreement between the experimental smooth silicon surface and the smooth fully diffuse simulation as seen in Figure 11. The experimental uncertainty, based on standard deviation, varies from about 10% at $P_0 < 200$Pa to less then 1% at $P_0 > 10{,}000$Pa. There is a 2% under-prediction by the DSMC simulations along the range of pressures tested. One of three effects can cause this deviation. The first is a finite specularity that may have

existed in the experiment and was unaccounted for in the simulations. The second is an uncertainty of approximately 2% in the area of the channel based on the SEM pictures. The third is the previously mentioned influence of surface absorption and the decrease of surface sites at higher pressures, also creating a higher physical specularity then accounted for in the simulation. However, relative influence of these effects are unknown. It is important to note that the pressure dependence of the under-prediction is hard to determine due to the larger experimental uncertainty at lower pressures.

There is also good agreement between the experimental triangular surface and the cone model simulations as seen in Figure 12. As with the smooth surface, the experimental uncertainty, based on standard deviation, varies from about 10% at $P_0 < 200$Pa to less then 1% at $P_0 > 10{,}000$Pa. At the higher pressures, there is less then 2% difference between the experiment and simulation; however, at the lower pressures, there is a 5% over-prediction by the DSMC. Again both the uncertainty in the experimental channel area and the larger statistical scatter at lower pressures could contribute to this difference.

The experimental data for the square surface features can be seen in Figure 13 compared with the other two experimental surfaces. Molecular interaction with the vertical walls of the square surfaces could be approximated as cones with opening angles $\beta=0°$. As expected, the square data falls between the smooth $\beta=180°$ and triangular $\beta=70°$ experimental points. Although the square surface data trends towards the triangular data at lower pressures, it moves towards the smooth data at higher pressures. This could be attributed to the influence of the exit plane on the flow and the reduction in Knudsen number as the pressure ratio increases. At higher pressures and densities, the square texture acts more like a fully diffuse surface then a series of

roughness features, until a few mean free paths before the exit plane, ultimately asymptoting at the smooth surface value.

V. CONCLUSION

A conical surface roughness model has been developed, numerically verified, and experimentally validated. For a particle simulation, the conical model reduces both setup and simulation time over direct geometric representation without sacrificing accuracy. For deterministic solvers, this conical model gives a crucial link between the Cercignani-Lampis (CL) scattering kernel, which requires a defined tangential momentum accommodation coefficient, α_t, and a physical surface characteristic, the average surface roughness angle. The conical model is general enough to be used for surfaces with both prescribed roughness features and non-uniform roughness features. In the latter case, a mix of conical opening angles and traditional diffuse interactions can be used based on the surface distribution.

Numerical simulations using the conical model, the CL scattering kernel, and a direct geometric representation of a regular triangular surface were compared against a smooth, fully diffuse model. All four cases were simulated with the DSMC method as two-dimensional flows of helium or nitrogen through a 150μm tall, 1.5cm long microchannel with Reynolds numbers from 0.01 to 10 based on inlet conditions. The direct geometric representation, the most costly but most accurate compared to experiment, showed a decrease in mass flow between 25% for the lower stagnation pressures simulated and 6% for the higher stagnation pressures simulated. The conical model matched this result to within 3% at the lower stagnation pressures and less than

1% for the higher stagnation pressures while the CL model matched this result within 7% and less than 1% respectively.

Experiments were conducted on transitional flows, where the mean free path is on the order of or larger than the roughness size, through a 1cm wide channel with similar height and length to the simulations to approximate 2-D conditions. The channel walls were made of silicon with: (i) polished smooth surfaces (ii) regular triangular roughness, and (iii) regular square roughness with characteristic roughness scales of <1μm, 11μm, and 29μm respectively. Experimental results validate the numerical simulations, which match to within 2% throughout the range tested for the smooth geometry and between 2% and 5% for the high and low stagnation pressures respectively for the triangular roughness geometry. The experimental mass flow for the square roughness geometry falls between the smooth and triangular cases over the entire test range as expected based on β.

VI. ACKNOWLEDGEMENTS

This work was supported by the U.S. Air Force Office of Scientific Research, administered by Dr. Mitat Birkan. Special thanks to Mr. Nathaniel Selden for his design of the textured silicon inserts which constitute the top and bottom of the experimental channel and Dr. Amish Desai at Tanner Research for his assistance in their manufacture. Also, thanks to Mr. Bruce Wilton at Mechanical Concepts for his assistance in the precision manufacture of the aluminum and Teflon components for the test assembly.

1 Veijola, T., "Model for Flow Resistance of a Rare Gas Accounting for Surface Roughness," Modeling and Simulation of Microsystems, NANOTECH 2003, San Francisco, February 2003, Vol. 2, pp. 492-495

2 Gaede, W., "Die innere Reibung der Gase," Ann. Physik, 41 (1913), 289-336

3 D.H. Davis, L.L. Levenson and N. Milleron, "Effects of 'rougher-than-rough' surfaces on molecular flow through short ducts," *J. Appl. Phys.* **35** (1964), pp. 529–532.

4 G.M. Mala and D. Li, "Flow characteristics of water in microtubes," *Int. J. Heat Mass Transfer* **20** (1999), pp. 142–148

5 Turner, S. E., Lam, C. C., Faghri, M., Gregory, O. J. " Experimental Investigation of Gas Flow in Microchannels," *Journal of Heat Transfer*, 2004, Vol. 126, pp. 753-764

6 C. Ngalande, T. Lilly, M. Killingsworth, S. Gimelshein, and A. Ketsdever, "Nozzle Plume Impingement on Spacecraft Surfaces: Effects of Surface Roughness," *J. of Spacecraft and Rockets*, Vol. 43, No. 5, pp. 1013-1018, 2006

7 Ji Y., Yuan K., Chung J.N., "Numerical simulation of wall roughness on gaseous flow and heat transfer in a microchannel," Int. J. Heat Mass Transfer, Vol. 49, 2006, pp. 1329-1339.

8 Ansumali et al, "Hydrodynamics beyond Navier-Stokes: Exact Solution to the Lattice Boltzmann Hierarchy," *Physical Review Letters*, Vol. 98, 2007, No. 124502

9 Ansumali, S. and Karlin, I, "Kinetic boundary conditions in the lattice Boltzmann method," *Physical Review E*, Vol. 66, 2002, pp. 26311

10 Cercignani, C, Lampis, M., "Kinetic models for gas-surface interactions," Trans. Theory and Stat. Phys., 1971, Vol. 1, No. 2, pp101-114

11 Benzi et al, "Mesoscopic modelling of heterogeneous boundary conditions for microchannel flows," *Journal of Fluid Mechanics*, Vol. 548, 2006, pp. 257-280

12 Sawada, T., Horie, B. Y., Sugiyama, W. “Diffuse scattering of gas molecules from conical surface roughness,” *Vacuum*, Volume. 47, No. 6-8, pp. 795-797, 1996

13 Sugiyama, W., Sawada, T., Yabuki, M., Chiba, Y. “Effects of surface roughness on gas flow conductance in channels estimated by a conical roughness model,” Applied Surface Science, 169-170, 2001, 787-791

14 F. Sharipov, “Application of the Cercignani–Lampis scattering kernel to calculations of rarefied gas flows.” II. Slip and jump coefficients. *European Journal of Mechanics B/Fluids*, Vol. 22, 2003, pp. 133-143.

15 Ketsdever A.D., Clabough M.T., Gimelshein S.F., Alexeenko A.A., “Experimental and Numerical Determination of Micropropulsion Device Efficiencies at Low Reynolds Numbers,” AIAA Journal, 2005, vol.43, no.3, pp.633-641.

16 H. Sun and M. Faghri, “Effect of Surface Roughness on Nitrogen Flow in a Microchannel Using the Direct Simulation Monte Carlo method.” Numerical Heat Transfer: Part A: Applications, Vol. 43, No. 1, January 2003, pp. 1-8.

17 Aksenova, O. A., Khalidov, I. A., “Fractal And Statistical Models Of Rough Surface Interaction With Rarified Gas Flow,” Proceedings of the 24th International Symposium on Rarefied Gas Dynamics, ed. M. Capitelli, (AIP, New York, 2005), pp. 993-998.

18 Aksenova, O. A., “The comparison of fractal and statistical models of surface roughness in the problem of scattering rarefied gas atoms,” Vestnik St. Petersburg University: Mathematics, Issue 1, 2004, pp. 61-66

19 Anolik, M.V., Kiulvari, I., “Direct modeling of gas atom reflection from a rough surface.” Aerodinamika Razrezhennykh Gazov, no. 7, 1974, p. 26-32.

20 Croce G., D'Agara P. "Numerical analysis of roughness effect on microtube heat transfer," Superlattices and Microstructures, Vol. 35, 2004, pp. 601-616.

21 Sugiyama, W., Sawadaa, T., Nakamori, K. "Rarefied gas flow between two flat plates with two dimensional surface roughness," *Vacuum*, 1996, Vol. 47, No. 6-8, pp.. 791-794

22 Borisov, S. F. "Progress in Gas-Surface Interaction Study," Proceedings of the 24th International Symposium on Rarefied Gas Dynamics, ed. M. Capitelli, (AIP, New York, 2005), pp. 933-940.

23 Lundstrom, I., Norberg, P., Petersson, L. G. "Wall-induced effects in gas transport through micromachined channels in silicon," *Journal of Applied Physics*, 1994, Vol. 76. pp. 142-147

24 Lord, R.G., "Some extensions to the Cercignani-Lampis gas-surface scattering kernel," *Phys. Fluids*, Vol. 3, April 1991, pp 706-710

25 Ivanov, M. S., Markelov, G. N., Gimelshein, S. F. "Statistical Simulation of Reactive Rarefied Flows: Numerical Approach Applications," AIAA Paper 98-2669, 31st AIAA Thermophysics Conference, Albuquerque, NM, June 1998

26 Ivanov, M. S., Rogasinsky, S. V., "Analysis of numerical techniques of the direct simulation Monte Carlo method in the rarefied gas dynamics," *Sov. J. Numer. Anal. Math. Modeling*, 1988, Vol. 3, No. 6, pp 453-465

Pressure Pa	Surface (i) kg/s	Surface (ii) kg/s	Surface (iii) kg/s	Surface (iv) kg/s
200	4.132E-09	3.188E-09	3.440E-09	3.093E-09
650	1.381E-08	1.125E-08	1.162E-08	1.105E-08
2000	5.680E-08	4.939E-08	4.997E-08	4.898E-08
4000	1.623E-07	1.484E-07	1.502E-07	1.483E-07
6000	3.094E-07	2.899E-07	2.893E-07	2.896E-07
8000	5.098E-07	4.810E-07	4.830E-07	4.810E-07

Table 1

Lilly

Table 1 Numerical results for mass flow as a function of stagnation pressure for various surface models using a helium test gas.

Figure 1 Schematic of new conical model reflection algorithm.

Figure 2 Distribution function of the angle between the reflected tangential velocity and the flow direction, M=0.3, β=66º.

Figure 3 Thermal relaxation of helium in a 300K box. Time is in mean collision times, τ_λ, at 1000K.

Figure 4 Tangential momentum accommodation coefficient, α_t, as a function of cone opening angle β, for M=0.3.

Figure 5 Tangential momentum accommodation coefficient, α_t as a function of Mach number for two cone opening angles.

Figure 6 Schematic of the computational domain.

Figure 7 Average experimental surface roughness feature dimensions for a) the triangular surface and b) the square surface.

Figure 8 SEM pictures of a) end of the triangular textures (from above), and b) view along cleaved square textures (from side).

Figure 9 Normalized pressure and Mach number as a function of distance downstream along the centerline for two stagnation conditions.

Figure 10 Pressure ratio as a function of distance downstream along the centerline, conical rough surface to smooth surface.

Figure 11 Comparison of the experimental smooth texture geometry and numerical smooth diffuse roughness model for a) helium gas, b) nitrogen gas.

Figure 12 Comparison of the experimental triangular texture geometry and numerical cone roughness model for a) helium gas, b) nitrogen gas.

Figure 13 Experimental results for the textured geometries for helium gas.

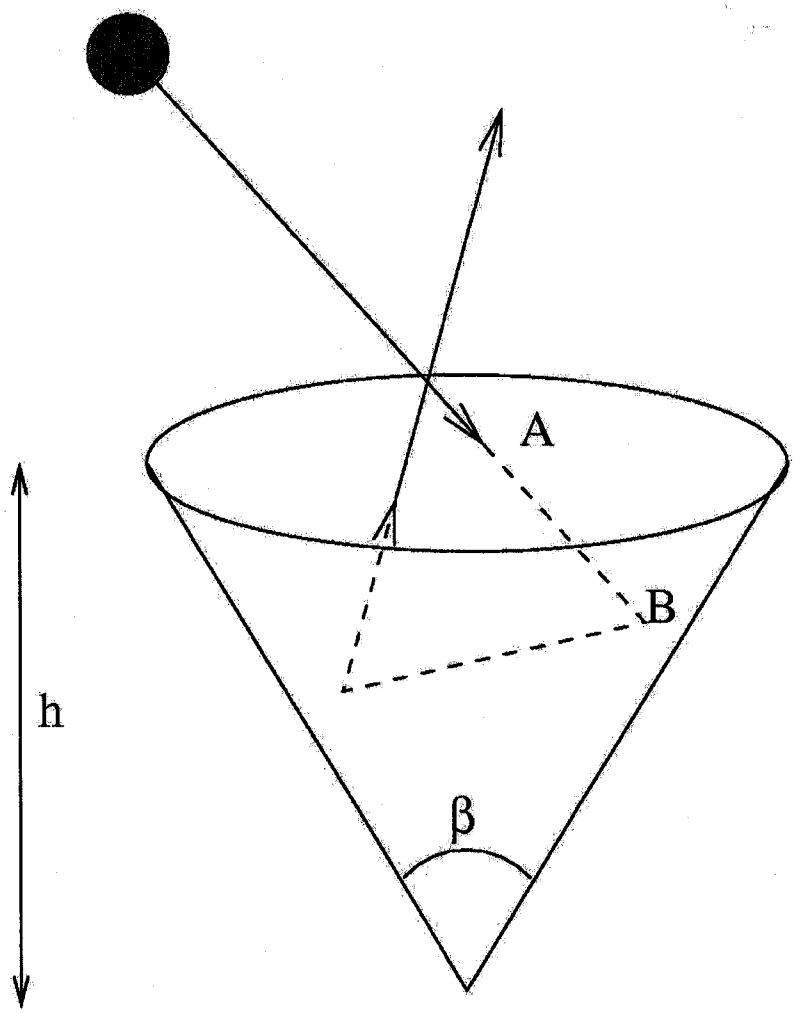

Figure 1

Lilly

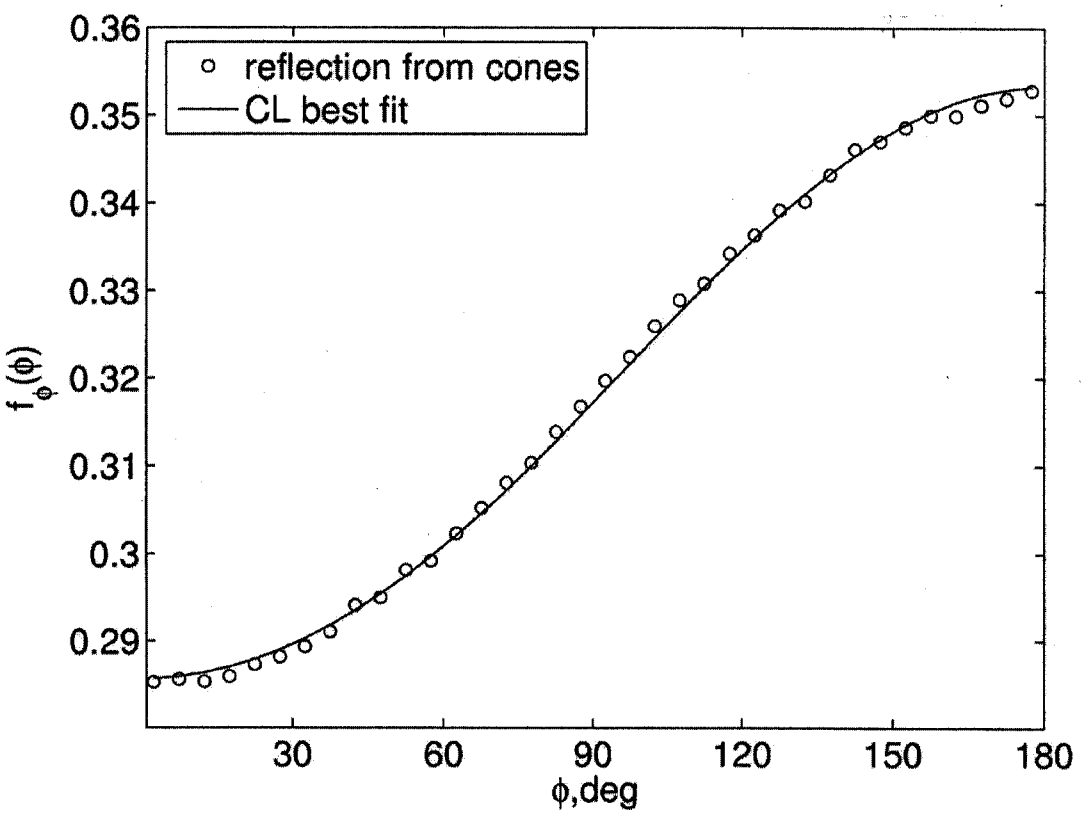

Figure 2

Lilly

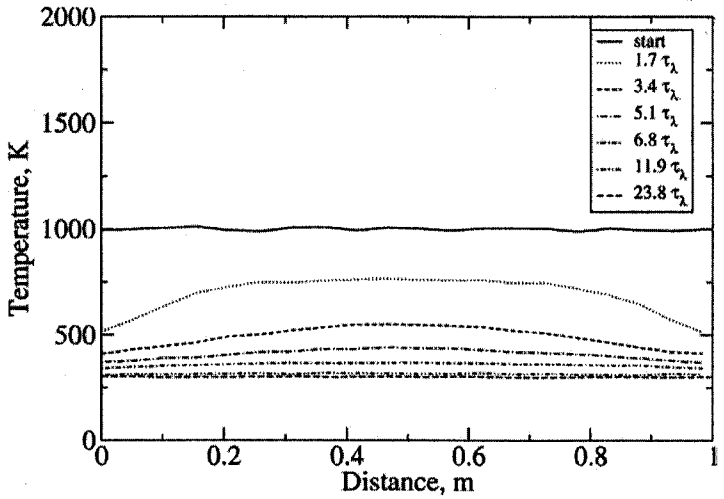

Figure 3

Lilly

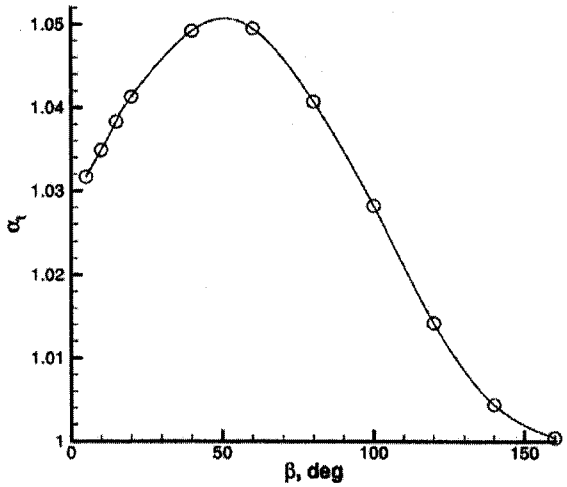

Figure 4

Lilly

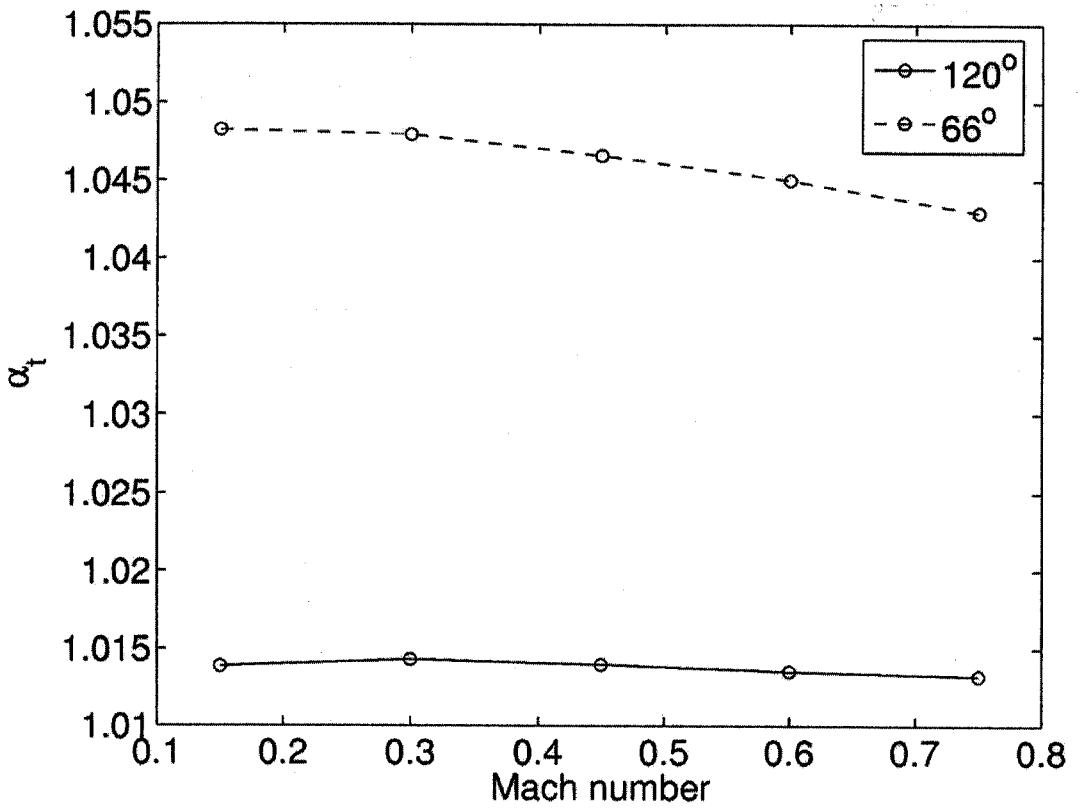

Figure 5

Lilly

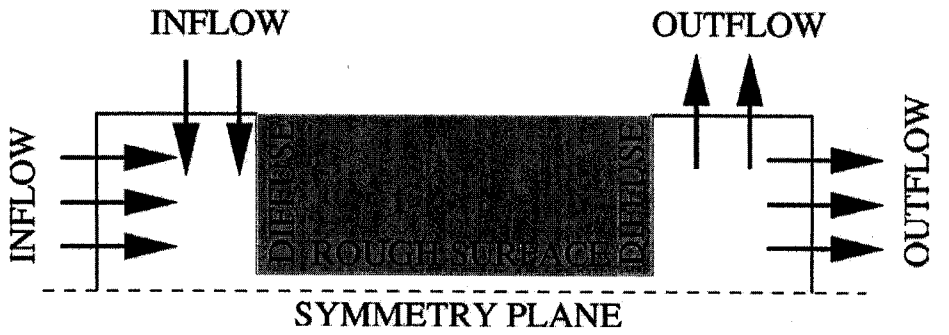

Figure 6

Lilly

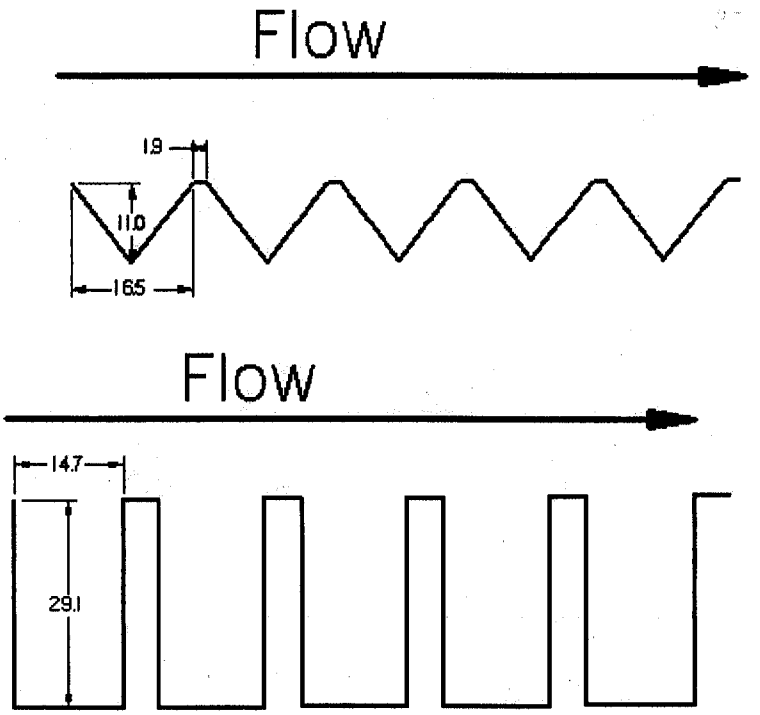

Figure 7

Lilly

A

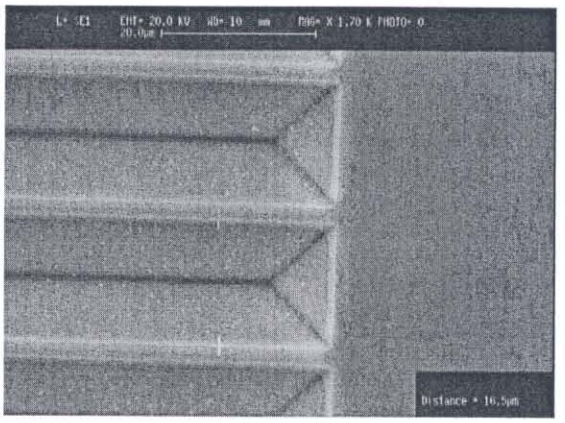

B

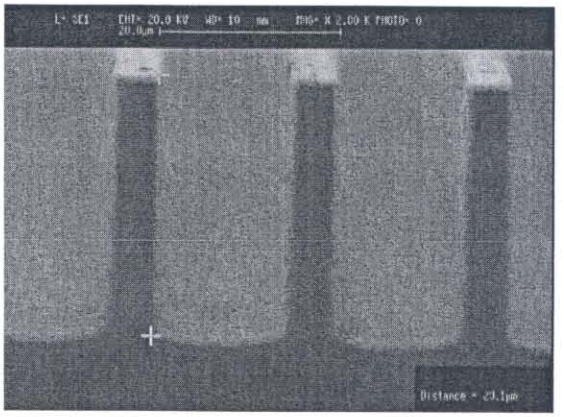

Figure 8

Lilly

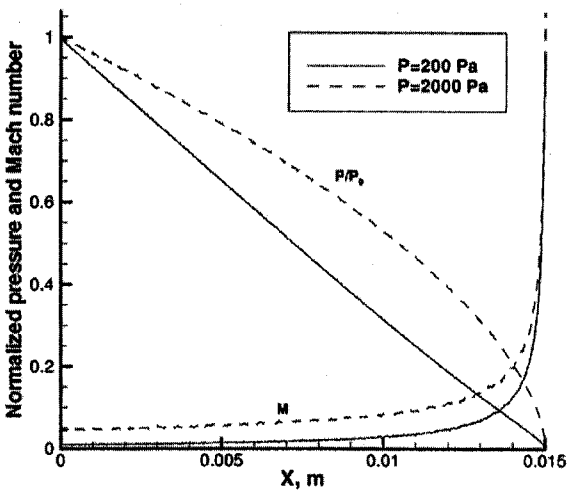

Figure 9

Lilly

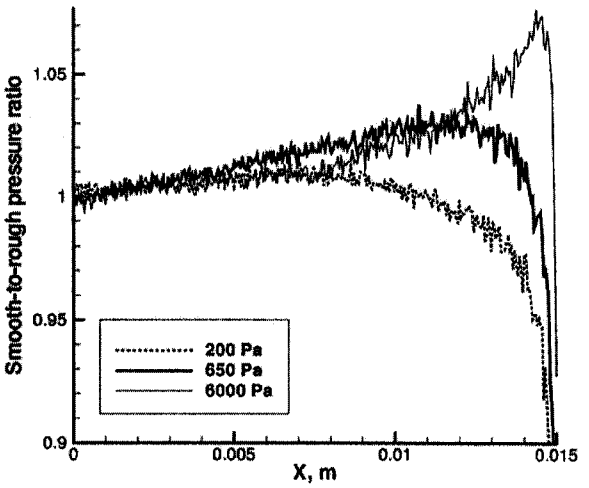

Figure 10

Lilly

A

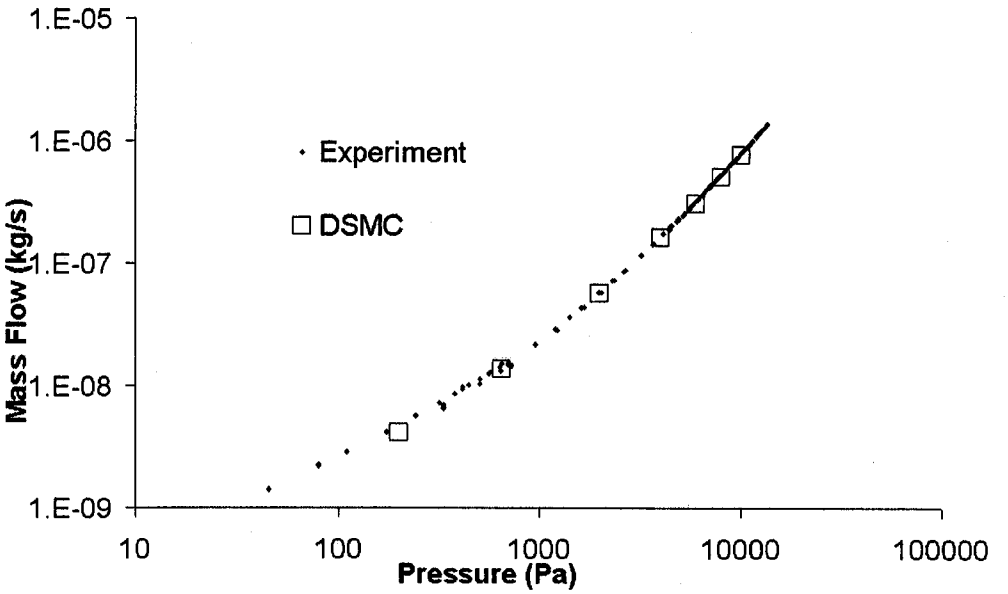

B

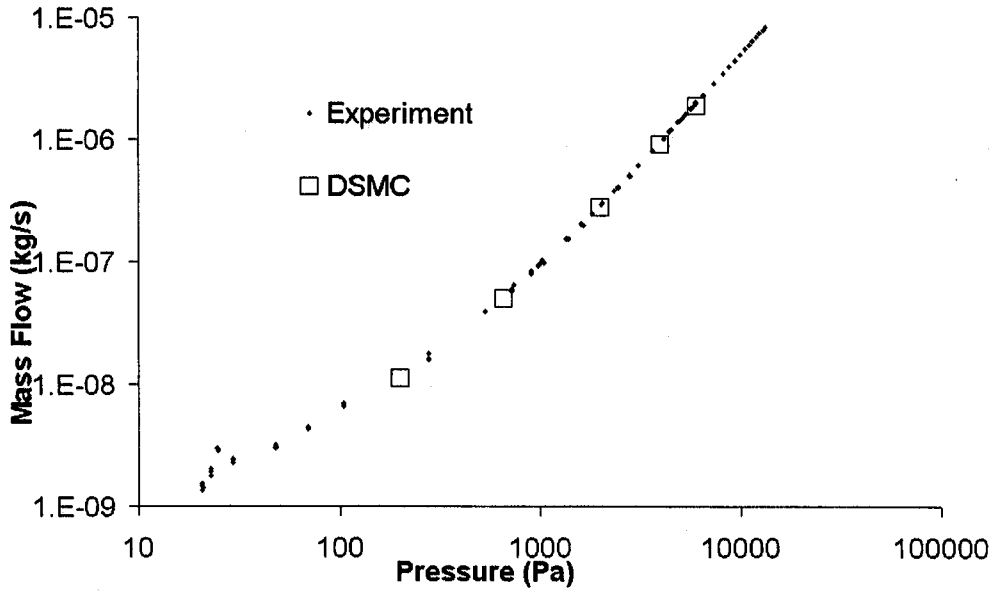

Figure 11

Lilly

A

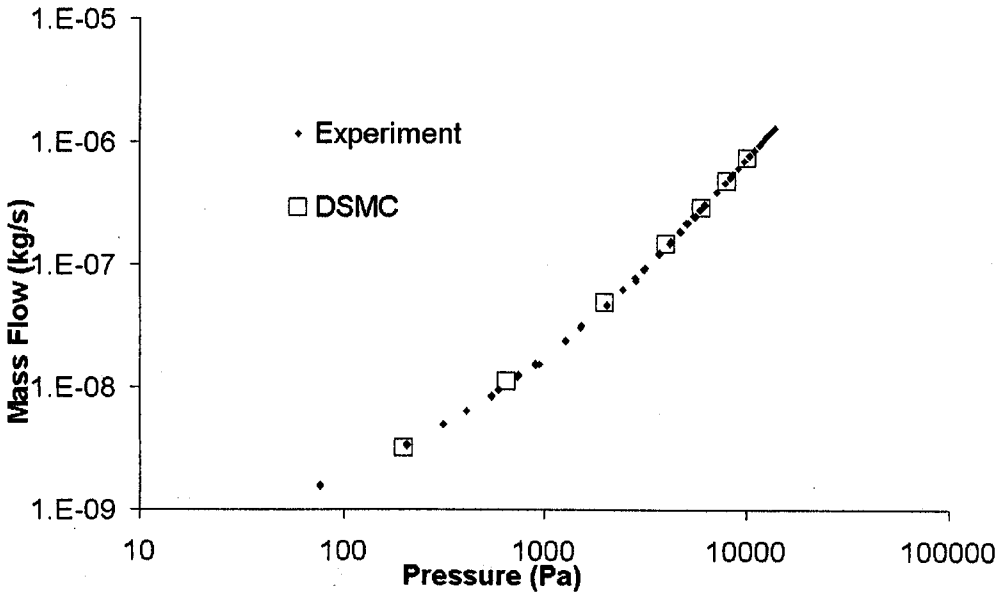

B

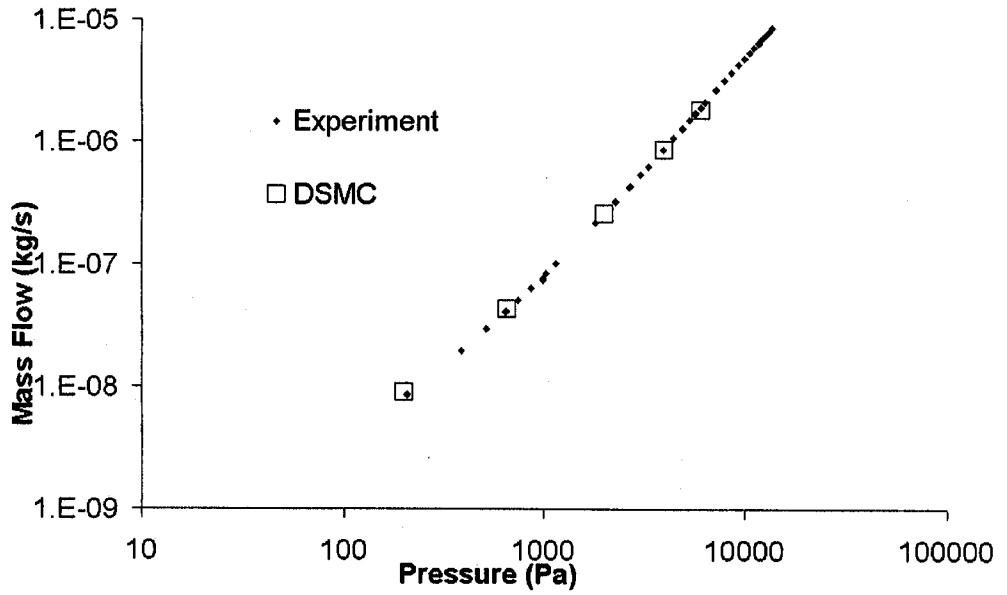

Figure 12

Lilly

A

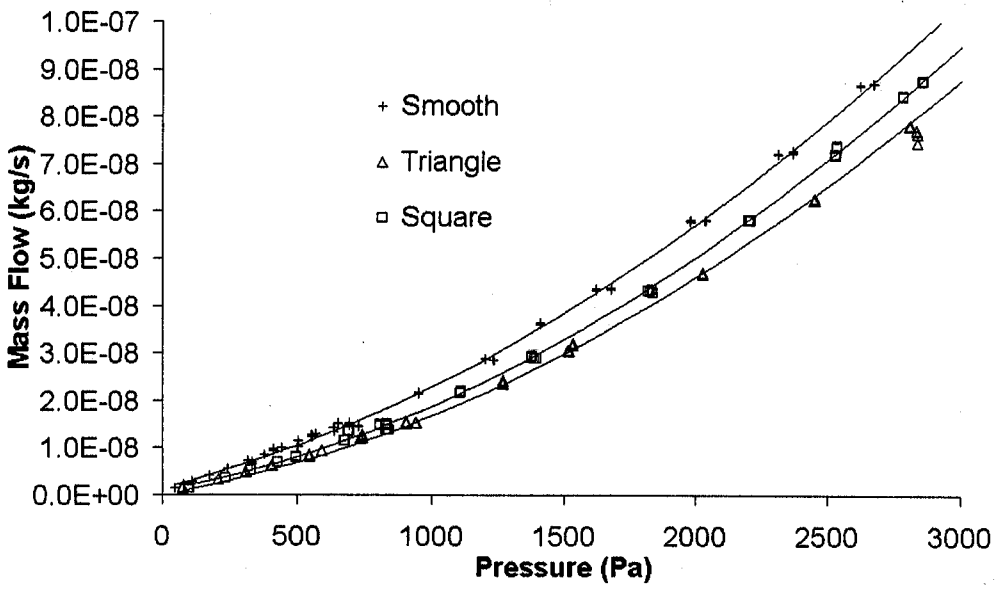

B

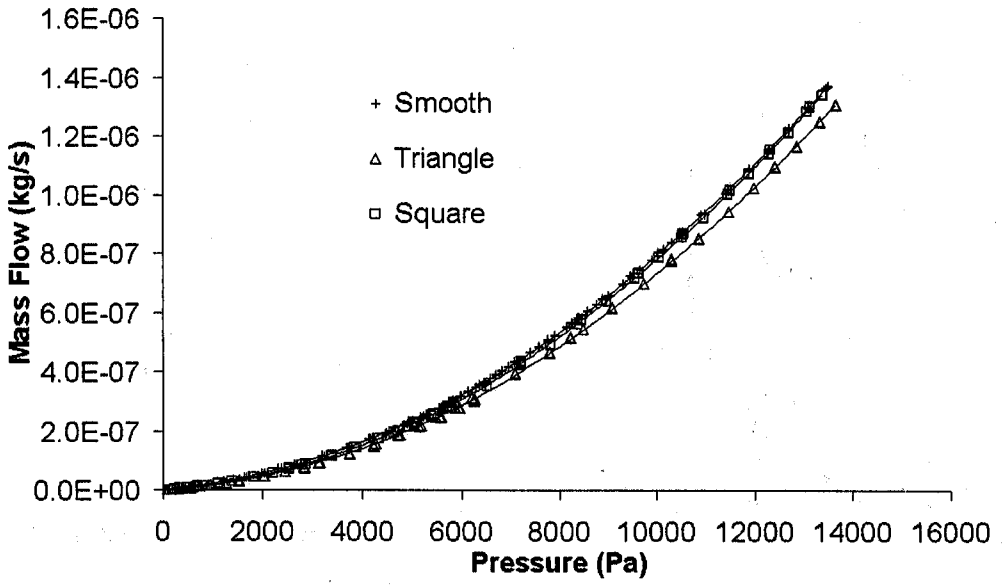

Figure 13

Lilly